
Amortized Bayesian inference for clustering models

Ari Pakman and Liam Paninski

Department of Statistics
 Center for Theoretical Neuroscience
 Grossman Center for the Statistics of Mind
 Columbia University

Abstract

We develop methods for efficient amortized approximate Bayesian inference over posterior distributions of probabilistic clustering models, such as Dirichlet process mixture models. The approach is based on mapping distributed, symmetry-invariant representations of cluster arrangements into conditional probabilities. The method parallelizes easily, yields iid samples from the approximate posterior of cluster assignments with the same computational cost of a single Gibbs sampler sweep, and can easily be applied to both conjugate and non-conjugate models, as training only requires samples from the generative model.

1 Introduction

Unsupervised clustering is a key tool in many areas of statistics and machine learning, and analyses based on probabilistic generative models are crucial whenever there is irreducible uncertainty about the number of clusters and their members.

Popular posterior inference methods in these models fall into two broad classes. On the one hand, MCMC methods [1, 2, 3] are asymptotically accurate but time-consuming, with convergence that is difficult to assess. Models whose likelihood and prior are non-conjugate are particularly challenging, since in these cases the model parameters cannot be marginalized and must be kept as part of the state of the Markov chain. On the other hand, variational methods [4, 5, 6] are typically much faster but do not come with accuracy guarantees.

In this work we propose a novel approximate amortized approach, based on training neural networks to map distributed, symmetry-invariant representations of cluster arrangements into conditional probabilities. The method can be applied to both conjugate and non-conjugate models, and after training the network with samples from a particular generative model, we can obtain independent, GPU-parallelizable, approximate posterior samples of cluster assignments for any new set of observations of arbitrary size, with no need for expensive MCMC steps.

2 The Neural Clustering Process

Probabilistic models for clustering [7] introduce random variables c_i denoting the cluster number to which the data point x_i is assigned, and assume a generating process of the form

$$c_1 \dots c_N \sim p(c_1, \dots, c_N) \quad (2.1)$$

$$\mu_k \sim p(\mu_k) \quad k = 1 \dots K \quad (2.2)$$

$$x_i \sim p(x_i | \mu_{c_i}) \quad i = 1 \dots N \quad (2.3)$$

Here K is the number of distinct values among the c_i 's, μ_k denotes a parameter vector controlling the distribution of the k -th cluster, and $p(c_{1:N})$ is assumed to be exchangeable. Examples of this

setting include Mixtures of Finite Mixtures [8] and many Bayesian nonparametric models, such as Dirichlet process mixture models (DPMM) (see [9] for a recent overview).

Given N data points $\mathbf{x} = \{x_i\}$, we are interested in sampling the c_i 's, using a decomposition

$$p(c_{1:N}|\mathbf{x}) = p(c_1|\mathbf{x})p(c_2|c_1, \mathbf{x}) \dots p(c_N|c_{1:N-1}, \mathbf{x}). \quad (2.4)$$

Note that $p(c_1|\mathbf{x}) = 1$, since the first data point is always assigned to the first cluster. To motivate our approach, it is useful to consider the joint distribution of the assignments of the first n data points,

$$p(c_1, \dots, c_n|\mathbf{x}). \quad (2.5)$$

We are interested in representations of \mathbf{x} that keep the symmetries of (2.5):

- **Permutations within a cluster:** (2.5) is invariant under permutations of x_i 's belonging to the same cluster. If there are K clusters, each of them can be represented by

$$H_k = \sum_{i:c_i=k} h(x_i) \quad k = 1 \dots K, \quad (2.6)$$

where $h : \mathbb{R}^{d_x} \rightarrow \mathbb{R}^{d_h}$ is a function we will learn from data. This type of encoding has been shown in [10] to be necessary to represent functions with permutation symmetries.

- **Permutations between clusters:** (2.5) is invariant under permutations of the cluster labels. In terms of the within-cluster invariants H_k , this symmetry can be captured by

$$G = \sum_{k=1}^K g(H_k), \quad (2.7)$$

where $g : \mathbb{R}^{d_h} \rightarrow \mathbb{R}^{d_g}$.

- **Permutations of the unassigned data points:** (2.5) is also invariant under permutations of the $N - n$ unassigned data points. This can be captured by

$$Q = \sum_{i=n+1}^N h(x_i). \quad (2.8)$$

Note that G and Q provide fixed-dimensional, symmetry-invariant representations of all the assigned and non-assigned data points, respectively, for any number of N data points and K clusters. Consider now the conditional distribution that interests us,

$$p(c_n|c_{1:n-1}, \mathbf{x}) = \frac{p(c_1 \dots c_n|\mathbf{x})}{\sum_{c'_n=1}^{K+1} p(c_1 \dots c'_n|\mathbf{x})}. \quad (2.9)$$

Assuming K different values in $c_{1:n-1}$, then c_n can take $K + 1$ values, corresponding to x_n joining any of the K existing clusters, or forming its own new cluster. Let us denote by G_k the value of (2.7) for each of these $K + 1$ configurations. In terms of the G_k 's and Q , we propose to model (2.9) as

$$p_\theta(c_n = k|c_{1:n-1}, \mathbf{x}) = \frac{e^{f(G_k, Q, h_n)}}{\sum_{k'=1}^{K+1} e^{f(G_{k'}, Q, h_n)}} \quad (2.10)$$

for $k = 1 \dots K + 1$, where $h_n = h(x_n)$ and θ denotes all the parameters in the functions h, g and f , that will be represented with neural networks. Note that this expression preserves the symmetries of the numerator and denominator in the rhs of (2.9). By storing and updating H_k and G for successive values of n , the computational cost of a full sample of $c_{1:N}$ is $O(NK)$, the same of a full Gibbs sweep. See Algorithm 1 for details; we term this approach the Neural Clustering Process (NCP).

2.1 Global permutation symmetry

There is yet another symmetry present in the lhs of (2.4) that is not evident in the rhs: a global simultaneous permutation of the c_i 's. If our model learns the correct form for the conditional probabilities, this symmetry should be (approximately) satisfied. We monitor this symmetry during training.

Algorithm 1 $O(NK)$ Neural Clustering Process Sampling

```

1:  $h_i \leftarrow h(x_i) \quad i = 1 \dots N$ 
2:  $Q \leftarrow \sum_{i=2}^N h_i$ 
3:  $H_1 \leftarrow h_1$ 
4:  $G \leftarrow g(H_1)$ 
5:  $K \leftarrow 1, c_1 \leftarrow 1$ 
6: for  $n \leftarrow 2 \dots N$  do
7:    $Q \leftarrow Q - h_n$ 
8:    $H_{K+1} \leftarrow 0$ 
9:   for  $k \leftarrow 1 \dots K + 1$  do
10:     $G \leftarrow G + g(H_k + h_n) - g(H_k)$ 
11:     $p_k \leftarrow e^{f(G, Q, h_n)}$ 
12:     $G \leftarrow G - g(H_k + h_n) + g(H_k)$ 
13:   end for
14:    $p_k \leftarrow p_k / \sum_{k'=1}^{K+1} p_{k'}$ 
15:    $c_n \sim p_k$ 
16:   if  $c_n = K + 1$  then
17:      $K \leftarrow K + 1$ 
18:   end if
19:    $G \leftarrow G - g(H_{c_n}) + g(H_{c_n} + h_n)$ 
20:    $H_{c_n} \leftarrow H_{c_n} + h_n$ 
21: end for
22: return  $c_1 \dots c_N$ 

```

▷ Initialize unassigned set
 ▷ Create first cluster with x_1
 ▷ Remove x_n from unassigned set
 ▷ We define $g(0) = 0$
 ▷ Add x_n
 ▷ Remove x_n
 ▷ Normalize probabilities
 ▷ Sample assignment for x_n
 ▷ Add point x_n

3 Learning

In order to learn the parameters θ , we use stochastic gradient descent to minimize the expected negative log-likelihood,

$$L(\theta) = -\mathbb{E}_{p(N)} \mathbb{E}_{p(c_1, \dots, c_N, \mathbf{x})} \mathbb{E}_{p(\pi)} \left[\sum_{n=2}^N \log p_\theta(c_{\pi_n} | c_{\pi_1: \pi_{n-1}}, \mathbf{x}) \right], \quad (3.1)$$

where $p(N)$ and $p(\pi)$ are uniform over a range of integers and over N -permutations, and samples from $p(c_1, \dots, c_N, \mathbf{x})$ are obtained from the generative model (2.1)-(2.3), irrespective of the model being conjugate. In Appendix C we show that (3.1) can be partially Rao-Blackwellized.

4 Related work

The work [11] provides an overview of deterministic clustering based on neural networks, and [12] proposes a biologically inspired network for online clustering. Our work differs from previous approaches in its use of neural networks to explicitly approximate fully Bayesian inference in a probabilistic generative clustering model. Similar amortized approaches to Bayesian inference have been explored in Bayesian networks [13], sequential Monte Carlo [14], probabilistic programming [15, 16] and particle tracking [17]. The representation of a set via a sum (or mean) of encoding vectors was also used in [10, 18, 19, 20].

5 Results

In this section we present examples of NCP clustering. The functions g and f have the same neural architecture in all cases, and for different data types we only change the encoding function h . More details are in Appendix A, where we also show that during training the variance of the joint likelihood (2.4) for different orderings of the data points drops to negligible values.

Figure 1 shows results for a DPMM of 2D conjugate Gaussians. In particular, we compare the estimated assignment probabilities for a last observation of a set, c_N , against their exact values, which are computable for conjugate models, showing excellent agreement.

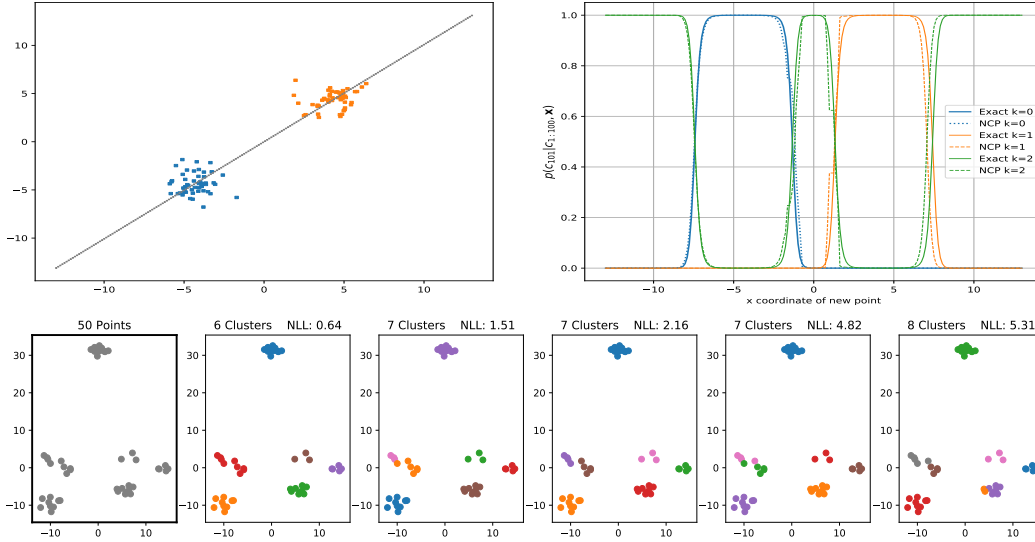


Figure 1: **NCP vs. exact posteriors.** *Upper left:* Two 2D clusters of 50 points each ($k = 0, 1$) and a line over possible locations of a 101st last point. *Upper right:* Assuming a DPMM (here with $\alpha = 0.7$, and 2D Gaussian observations with unit variance and mean with a prior $N(0, \sigma_\mu = 10 \times \mathbf{1}_2)$), the posterior $p(c_{101}|c_{1:100}, \mathbf{x})$ can be computed exactly, and we compare it to the NCP estimate as a function of the horizontal coordinate of x_{101} , as this point moves over the gray line on the upper left panel. *Lower:* Five samples from the posterior of the same 2D model, given the observations in the leftmost panel. In each sample, the order of the particles was randomly shuffled. Note that the posterior samples are reasonable, and less-reasonable samples are assigned higher negative log-likelihood (NLL) values by the NCP. (Best seen in color.)

Figure 2 shows results for a DPMM over the empirical distribution of 28×28 -pixel handwritten digits from the MNIST dataset. In this case the generative model has no analytical expression. The results show that the NCP samples correctly capture the label ambiguity of some of the digits.

K	NLL	8	8	8	8	8	9	9	9	9	7	7	7	7	7	7	7	0	6	
5	0.38	1	1	1	1	1	1	2	2	2	2	3	3	3	3	3	3	3	4	5
4	2.23	1	1	1	1	1	1	2	2	2	2	3	3	3	3	3	3	3	4	4
4	2.77	1	1	1	1	1	1	2	2	2	2	3	3	3	3	3	3	3	4	1
5	4.00	1	1	1	1	4	1	2	2	2	2	3	3	3	3	3	3	3	4	5
5	5.07	1	1	1	1	5	1	2	2	2	2	3	3	3	3	3	3	3	4	5
4	5.81	1	1	1	1	4	1	2	2	2	2	3	3	3	3	3	3	3	4	4

Figure 2: **Clustering of MNIST data.** The generative model is a DPMM with concentration parameter $\alpha = 0.7$ and a uniform discrete base measure over the 10 labels. Conditioned on a label, observations are sampled uniformly from the MNIST training set. The figure shows $N = 20$ observations, generated similarly from the MNIST test set. The six rows below the observations show six samples of $c_{1:20}$ from the NCP posterior of these 20 images. Most samples from the NCP yield the first row of assignments, which has very low negative-loglikelihood (NLL) and is consistent with the true labels. The next five rows correspond to more rare samples from the NCP, with higher NLL, each capturing some ambiguity suggested by the form of particular digits. In this case we drew 39 samples: 34 corresponding to the first row, and one to each of the next five rows.

6 Outlook

We have introduced a new approach to sample from (approximate) posterior distributions of probabilistic clustering models. Our first results show reasonable agreement with Gibbs sampling, with major improvements in speed and model flexibility.

A Details of the examples

We implemented the functions g and f as six-layered MLPs with PReLU non-linearities [21], with 128 neurons in each layer, and final layers of dimensions $d_g = 512$ for g and 1 for f . We used stochastic gradient descent with ADAM [22], with a step-size of 10^{-4} for the first 1000 iterations, and 10^{-5} afterwards. The number of Monte Carlo samples from (3.1) in each mini-batch were: 1 for $p(N)$, 8 for $p(\pi)$, 1 for $p(c_{1:N})$ and 48 for $p(\mu_k)$ and $p(\mathbf{x}|\mu)$.

A.1 Low-dimensional conjugate Gaussian models

The generative model for the examples in Figure 1 is

$$N \sim \text{Uniform}[5, 100] \quad (\text{A.1})$$

$$c_1 \dots c_N \sim \text{DPMM}(\alpha) \quad (\text{A.2})$$

$$\mu_k \sim N(0, \sigma_\mu^2 \mathbf{1}_2) \quad k = 1 \dots K \quad (\text{A.3})$$

$$x_i \sim N(\mu_{c_i}, \sigma^2 \mathbf{1}_2) \quad i = 1 \dots N \quad (\text{A.4})$$

with $\alpha = 0.7$, $\sigma_\mu = 10$, $\sigma = 1$, and $d_x = 2$. The encoding function $h(x)$ is a five-layered MLPs with PReLU non-linearities, with 128 neurons in the inner layers and a last layer with $d_h = 256$ neurons.

A.2 High-dimensional MNIST data

The generative model for the example in Figure 2 is

$$N \sim \text{Uniform}[5, 100] \quad (\text{A.5})$$

$$c_1 \dots c_N \sim \text{DPMM}(\alpha) \quad (\text{A.6})$$

$$l_k \sim \text{Uniform}[0, 9] \quad k = 1 \dots K \quad (\text{A.7})$$

$$x_i \sim \text{Uniform}[\text{MNIST digits with label } l_{c_i}] \quad i = 1 \dots N \quad (\text{A.8})$$

with $\alpha = 0.7$, $d_x = 28 \times 28$. The architecture for $h(x)$ was: two layers of [convolutional + maxpool + ReLU] followed by [fully connected(256) + ReLU + fully connected(d_h)], with $d_h = 256$.

A.3 Invariance under global permutations

As mentioned in Section 2.1, if the conditional probabilities (2.9) are learned correctly, invariance of the joint probability (2.4) under global permutations should hold. Figure 3 shows estimates of the variance of the joint probability under permutations as learning progresses, showing that it diminishes to negligible values.

B Importance Sampling

Samples from the NCP can be used either as approximate samples from the posterior, or as high-quality importance samples. (Alternatively, we could use samples from the NCP to seed an exact MCMC sampler; we have not yet explored this direction systematically.) In the latter case, the expectation of a function $r(\mathbf{c})$ is given by

$$\mathbb{E}_{p(\mathbf{c}|\mathbf{x})} [r(\mathbf{c})] \simeq \frac{\sum_{s=1}^S \frac{p(\mathbf{c}_s, \mathbf{x})}{p_\theta(\mathbf{c}_s|\mathbf{x})} r(\mathbf{c}_s)}{\sum_{s=1}^S \frac{p(\mathbf{c}_s, \mathbf{x})}{p_\theta(\mathbf{c}_s|\mathbf{x})}} \quad (\text{B.1})$$

where each \mathbf{c}_s is a sample from $p_\theta(\mathbf{c}|\mathbf{x})$. Figure 4 shows a comparison between an expectation obtained from Gibbs samples vs importance NCP samples.

C Rao-Blackwellization

With some more computational effort, it is possible to partially Rao-Blackwellize the expectation in (3.1) and reduce its variance.

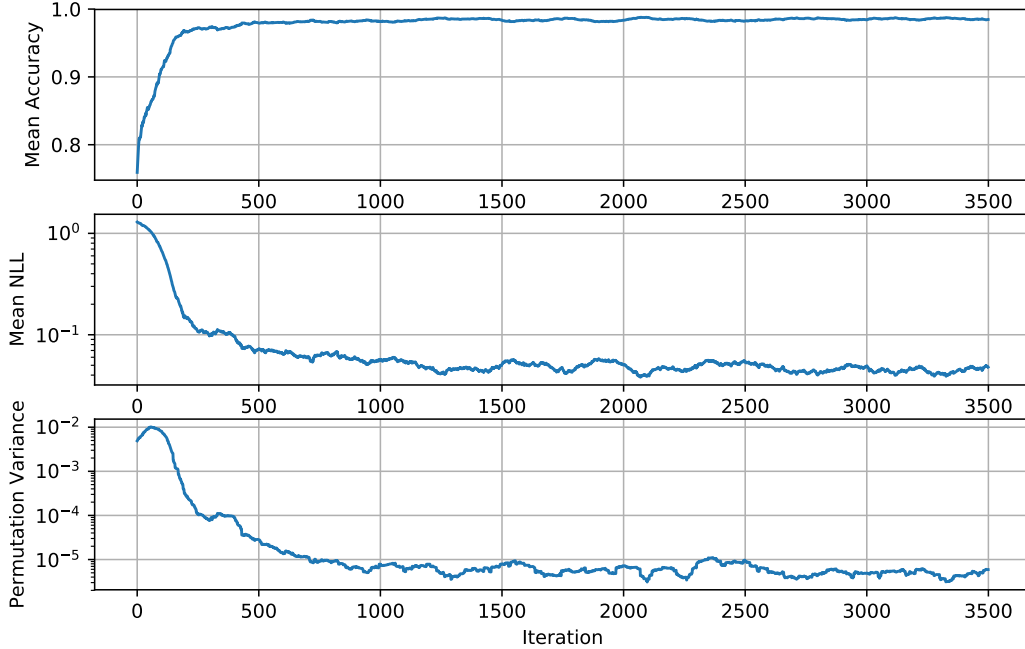


Figure 3: All the curves correspond to training of the 2D model described in Figure 1. To ease the visualization, we show the averages of a sliding window of 100 previous iterations. *Top*: ‘Accuracy’ measures the fraction of the cluster labels in the training samples that agree with the the maximum of the learned categorical distribution. *Center*: Mean negative log-likelihood in logarithmic scale. *Bottom*: Variance of the joint log likelihood under global permutations, estimated from 8 random permutations, in logarithmic scale.

C.1 Conjugate Models

For given N and \mathbf{x} , a generic term in (3.1) can be written is

$$\begin{aligned} \sum_{\mathbf{c}} p(\mathbf{c}|\mathbf{x}) \log p_{\theta}(c_n|c_{1:n-1}, \mathbf{x}) &= \sum_{\mathbf{c}} p(c_{n:N}|c_{1:n-1}, \mathbf{x}) p(c_{1:n-1}|\mathbf{x}) \log p_{\theta}(c_n|c_{1:n-1}, \mathbf{x}) \\ &\approx \sum_{c_{n:N}} p(c_{n:N}|c_{1:n-1}, \mathbf{x}) \log p_{\theta}(c_n|c_{1:n-1}, \mathbf{x}) \end{aligned} \quad (\text{C.1})$$

$$= \sum_{c_n} p(c_n|c_{1:n-1}, \mathbf{x}) \log p_{\theta}(c_n|c_{1:n-1}, \mathbf{x}) \quad (\text{C.2})$$

where we took here $\pi_i = i$ to simplify the notation. In (C.1) we replaced the expectation under $p(c_{1:n-1}|\mathbf{x})$ with a sample of $c_{1:n-1}$, and in (C.2) we summed over $c_{n+1:N}$. The expectation in (C.2) has lower variance than using a sample of c_n instead.

If there are K different values in $c_{1:n-1}$, we need to compute about $(K+1)(K+2)\dots(K+N-n+1)$ values for $p(c_{n:N}|c_{1:n-1}, \mathbf{x})$ in (C.1), corresponding to all the values the set $c_{n:N}$ can take. Each of these can be computed by evaluating

$$p(c_{n:N}|c_{1:n-1}, \mathbf{x}) \propto p(\mathbf{c})p(\mathbf{x}|\mathbf{c}) \quad (\text{C.3})$$

with $c_{1:n-1}$ fixed, and then normalizing. Below we present an example of this computation.

Moreover, after computing $p(\mathbf{c})p(\mathbf{x}|\mathbf{c})$ for fixed $c_{1:n-1}$ and all $c_{n:N}$, we can similarly Rao-Blackwellize all the other $N-n$ terms with $p(c_{n+1}|c_{1:n}, \mathbf{x}), \dots, p(c_N|c_{1:N-1}, \mathbf{x})$. Each of these distributions can be obtained from our original evaluation of $p(\mathbf{c})p(\mathbf{x}|\mathbf{c})$, by fixing the conditioning \mathbf{c}' s and summing over the others.

Example: DPMM with 1D Gaussian likelihood and Gaussian prior for the mean

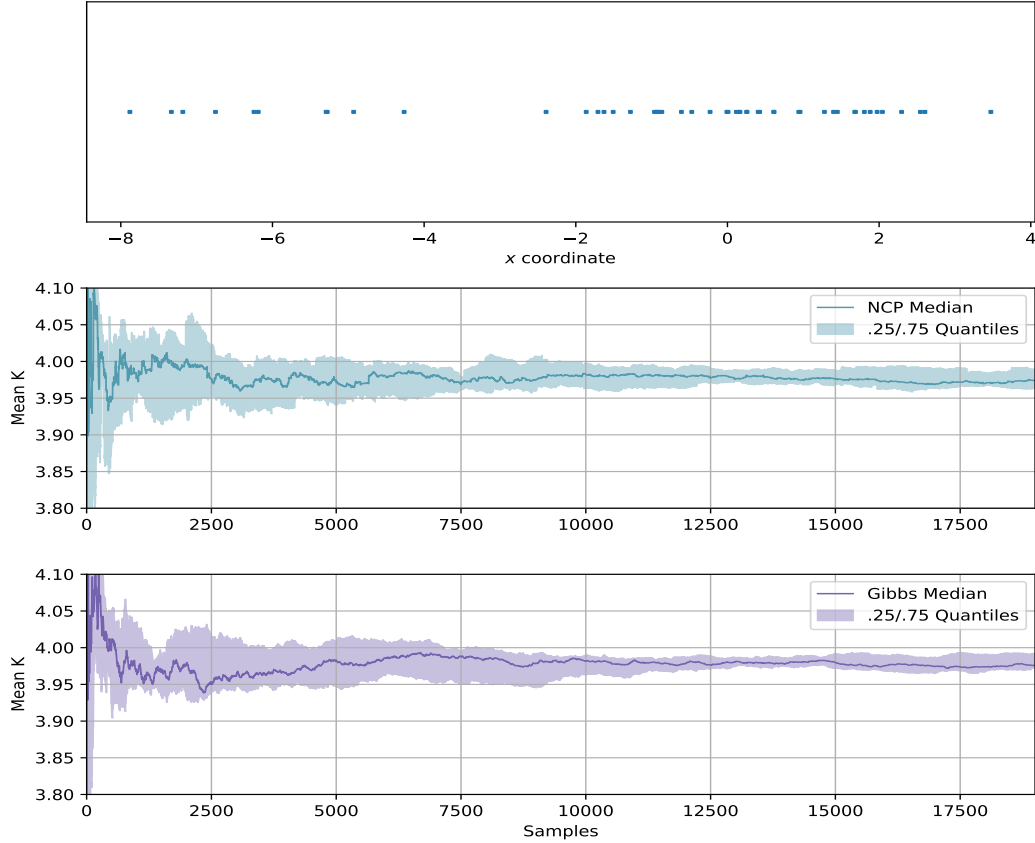


Figure 4: **Gibbs vs NCP importance sampling.** We assume a 1D generative model similar to the 2D model of Figure 1, and compute the mean of the number of clusters K as a function of the number of samples, for the dataset of $N = 50$ observations in the upper panel. The figures show medians and 0.25/0.75 quantiles for eight repetitions. In this simple example the variance of Gibbs and NCP are comparable, but the average CPU/GPU running time was 184 secs. for each NCP run of 20,000 samples, and 1969 secs. for each Gibbs run (with additional 1000 burn-in samples). The time advantage of NCP is due to the fact that since all samples are iid, NCP can be massively parallelized over GPUs, while in naive implementations of the Gibbs sampler the samples must be obtained sequentially.

The observation model is

$$p(\mu|\lambda) = N(0, \sigma_\mu^2 = \lambda^2) \quad (\text{C.4})$$

$$p(x|\mu, \sigma) = N(\mu, \sigma_x^2 = \sigma^2) \quad (\text{C.5})$$

with λ and σ fixed. In this case we get

$$p(\mathbf{x}|c) = \prod_{k=1}^K \int d\mu_k N(\mu_k|0, \lambda^2) \prod_{i:c_i=k} N(x_i|\mu_k, \sigma^2) \quad (\text{C.6})$$

$$= \prod_{k=1}^K \frac{\sigma_k}{\lambda} \exp\left(\frac{\sigma_k^2 (\sum_{i_k} x_{i_k})^2}{2\sigma^4}\right) \exp\left(-\frac{\sum_{i_k} x_{i_k}^2}{2\sigma^2}\right) \quad (\text{C.7})$$

where $\{i_k\} = \{i : c_i = k\}$ and $\sigma_k^{-2} = \lambda^{-2} + n_k \sigma^{-2}$, with $n_k = |i_k|$, and

$$p(c_{1:N}) = \frac{\alpha^{K_N} \prod_{k=1}^{K_N} (n_k - 1)!}{\prod_{i=1}^N (i - 1 + \alpha)} \quad (\text{C.8})$$

with α the Dirichlet process concentration parameter.

C.2 Nonconjugate Case

This case is similar, using

$$\begin{aligned}
 \sum_{\mathbf{c}} p(\mathbf{c}|\mathbf{x}) \log p_{\theta}(c_n|c_{1:n-1}, \mathbf{x}) &= \sum_{\mathbf{c}} \int d\mu p(\mathbf{c}, \mu|\mathbf{x}) \log p_{\theta}(c_n|c_{1:n-1}, \mathbf{x}) \\
 &= \sum_{\mathbf{c}} \int d\mu p(c_{n:N}|c_{1:n-1}, \mu, \mathbf{x}) p(c_{1:n-1}, \mu|\mathbf{x}) \log p_{\theta}(c_n|c_{1:n-1}, \mathbf{x}) \\
 &\simeq \sum_{c_{n:N}} p(c_{n:N}|c_{1:n-1}, \mu, \mathbf{x}) \log p_{\theta}(c_n|c_{1:n-1}, \mathbf{x}) \quad (\text{C.9}) \\
 &= \sum_{c_n} p(c_n|c_{1:n-1}, \mu, \mathbf{x}) \log p_{\theta}(c_n|c_{1:n-1}, \mathbf{x}) \quad (\text{C.10})
 \end{aligned}$$

where now in (C.9) we replaced the expectation under $p(c_{1:n-1}, \mu|\mathbf{x})$ with samples of $c_{1:n-1}, \mu$. In this case we need to evaluate

$$p(c_{N-r+1:N}|\mu, c_{1:N-r}, \mathbf{x}) \propto p(c_{N-r+1:N}, \mathbf{x}|\mu, c_{1:N-r}) \quad (\text{C.11})$$

$$= p(c_{N-r+1:N}|c_{1:N-r}) p(\mathbf{x}|\mu, c_{1:N}). \quad (\text{C.12})$$

Acknowledgments

This work was supported by the Simons Foundation, the DARPA NESD program, and by ONR N00014-17-1-2843.

References

- [1] Radford M Neal. Markov chain sampling methods for Dirichlet process mixture models. *Journal of computational and graphical statistics*, 9(2):249–265, 2000.
- [2] Sonia Jain and Radford M Neal. A split-merge Markov chain Monte Carlo procedure for the Dirichlet process mixture model. *Journal of computational and Graphical Statistics*, 13(1):158–182, 2004.
- [3] Sonia Jain, Radford M Neal, et al. Splitting and merging components of a nonconjugate dirichlet process mixture model. *Bayesian Analysis*, 2(3):445–472, 2007.
- [4] David M. Blei and Michael I. Jordan. Variational Methods for the Dirichlet Process. In *Proceedings of the Twenty-first International Conference on Machine Learning, ICML '04*, pages 12–, New York, NY, USA, 2004. ACM.
- [5] Kenichi Kurihara, Max Welling, and Yee Whye Teh. Collapsed Variational Dirichlet Process Mixture Models. In *IJCAI*, volume 7, pages 2796–2801, 2007.
- [6] Michael Hughes, Dae Il Kim, and Erik Sudderth. Reliable and scalable variational inference for the hierarchical Dirichlet process. In *Artificial Intelligence and Statistics*, pages 370–378, 2015.
- [7] Geoffrey J McLachlan and Kaye E Basford. *Mixture models: Inference and applications to clustering*, volume 84. Marcel Dekker, 1988.
- [8] Jeffrey W Miller and Matthew T Harrison. Mixture models with a prior on the number of components. *Journal of the American Statistical Association*, 113(521):340–356, 2018.
- [9] Abel Rodriguez and Peter Müller. NONPARAMETRIC BAYESIAN INFERENCE. *NSF-CBMS Regional Conference Series in Probability and Statistics*, 9:i–110, 2013.
- [10] Manzil Zaheer, Satwik Kottur, Siamak Ravanbakhsh, Barnabás Póczos, Ruslan Salakhutdinov, and Alexander J. Smola. Deep sets. In *Advances in neural information processing systems*, 2017.
- [11] K-L Du. Clustering: A neural network approach. *Neural networks*, 23(1):89–107, 2010.
- [12] Cengiz Pehlevan, Alexander Genkin, and Dmitri B. Chklovskii. A clustering neural network model of insect olfaction. *bioRxiv*, 2018.
- [13] Andreas Stuhlmüller, Jacob Taylor, and Noah Goodman. Learning stochastic inverses. In *Advances in neural information processing systems*, pages 3048–3056, 2013.
- [14] Brooks Paige and Frank Wood. Inference networks for sequential Monte Carlo in graphical models. In *International Conference on Machine Learning*, pages 3040–3049, 2016.
- [15] Daniel Ritchie, Paul Horsfall, and Noah D Goodman. Deep amortized inference for probabilistic programs. *arXiv preprint arXiv:1610.05735*, 2016.
- [16] Tuan Anh Le, Atilim Gunes Baydin, and Frank Wood. Inference compilation and universal probabilistic programming. *arXiv preprint arXiv:1610.09900*, 2016.
- [17] Ruoxi Sun and Liam Paninski. Scalable approximate Bayesian inference for particle tracking data. In *Proceedings of the 35th International Conference on Machine Learning*, 2018.
- [18] Harrison Edwards and Amos Storkey. Towards a neural statistician. *ICLR*, 2017.
- [19] Marta Garnelo, Dan Rosenbaum, Chris J Maddison, Tiago Ramalho, David Saxton, Murray Shanahan, Yee Whye Teh, Danilo J Rezende, and SM Eslami. Conditional neural processes. In *International Conference on Machine Learning*, 2018.
- [20] Marta Garnelo, Jonathan Schwarz, Dan Rosenbaum, Fabio Viola, Danilo J Rezende, SM Eslami, and Yee Whye Teh. Neural processes. In *ICML 2018 workshop on Theoretical Foundations and Applications of Deep Generative Models*, 2018.
- [21] Bing Xu, Naiyan Wang, Tianqi Chen, and Mu Li. Empirical evaluation of rectified activations in convolutional network. *arXiv preprint arXiv:1505.00853*, 2015.
- [22] Diederik P Kingma and Jimmy Ba. Adam: A method for stochastic optimization. *ICLR*, 2015.